J Electroceram (2009) 22:171–179
DOI 10.1007/s10832-007-9361-6

Materials, structures and power interfaces for efficient piezoelectric energy harvesting

Elie Lefeuvre · Gaël Sebald · Daniel Guyomar · Mickaël Lallart · Claude Richard

Received: 27 March 2007 / Accepted: 7 November 2007 / Published online: 22 November 2007

Abstract The possibility of recycling ambient energies with miniature electrical generators instead of using batteries with limited lifespan has stimulated important research efforts over the past years. Integration of such miniature generators is mainly envisioned into low power autonomous systems, for various industrial or domestic applications. This paper focuses on the use of piezoelectric materials for generating electrical energy from ambient mechanical vibrations. A review of the piezoelectric materials and the electromechanical structures which have been proposed in this field is first presented. Electrical circuits with one-stage, two-stage and three-stage interfaces which have been developed for optimizing the electrical power flow from piezoelectric devices to energy storage elements are then compared to a novel technique for controlling the energy converted by piezoelectric materials. This novel approach is derived from Ericsson thermodynamic cycle. A solution for practical implementation is proposed, theoretical predictions and experimental results are compared and discussed.

Keywords Piezoelectric · Vibration · Energy harvesting · Energy scavenging · Power optimization

1 Introduction

Permanent proliferation of wireless and mobile electronic devices creates an increasing demand for miniature electrical generators for domestic, industrial, military or spatial applications. The possibility of recycling ambient energies and getting electrical generators with unlimited lifetime is of major interest, as well as from practical and economic points of view or from the resources conservation point of view. That is why materials and devices for converting ambient energies into electricity have received a great deal of interest in research communities over the past few years.

In this paper, we propose an analysis of the energy converted by piezoelectric materials used in miniature electrical generators. Such devices, so-called "energy harvesters", recycle the ambient vibrations which may take place in many kind of environments. The most important physical characteristics of piezoelectric materials used for energy harvesting are first discussed. Then, a single degree of freedom model which may faithfully describe most of the electromechanical structures of piezoelectric energy harvesting devices is presented. This paper focuses in particular on the electrical interfaces which are connected between the piezoelectric electrodes and the electronic load using the electrical energy produced by the generator. The need for such interfaces comes from the fact that the electronic loads and the components which may be used for energy storage require DC voltages, whereas the piezoelectric elements produce AC voltages. Moreover, the desired outputs may need to be accurately regulated. Recent works showed also that such interfaces have a strong influence on the energy converted by the piezoelectric materials [1, 2, 4, 5, 10–13]. Energy conversion cycles of piezoelectric materials using one-stage, two-stage and three-stage power interfaces are presented and compared to a new technique derived from Ericsson thermodynamic cycle. Finally, solutions for practical implementation of these interfaces are proposed and experimental results obtained using each interface are presented and discussed.

E. Lefeuvre (✉) · G. Sebald · D. Guyomar · M. Lallart · C. Richard
INSA-Lyon, LGEF Laboratory,
8 rue de la physique,
69621 Villeurbanne, France
e-mail: elie.lefeuvre@insa-lyon.fr

2 Piezoelectric materials

Owing to their electromechanical properties, piezoelectric materials are very good candidates for converting into electrical energy the energy provided by vibrations. A large variety of piezoelectric ceramics, single crystals and composites are now available, enabling the design of vibration-powered PEGs (Piezoelectric Electrical Generators) with various shapes and dimensions. Previous works on PEGs have highlighted some of the most important piezoelectric characteristics to be considered for selecting active materials. The electromechanical coupling coefficient k can be considered as one of the most important parameter since it directly quantifies the ability for energy conversion. The longitudinal coupling coefficient k_{33} and the transverse coupling coefficient k_{31} determine in particular the most effective use of a given active material, that is to say the poling axis direction, the stress main axis and the disposition of the electrodes for optimal use of the material. Another important parameter is the mechanical quality factor Q_m which is related to the mechanical losses. It is clear that the mechanical losses of an energy harvesting device must be as low as possible for converting as much mechanical energy as possible into electricity. The figure of merit for energy conversion in resonant devices can be defined as the product of the squared coupling coefficient and the mechanical quality factor: k^2Q_m. The material figure of merit is of course different from the figure of merit of the electromechanical system, the latter being defined by the product of the overall squared coupling coefficient and the overall quality factor of the device. The maximal stress and strain the materials can accept are also very important parameters to be considered, in order to avoid irreversible alterations. The piezoelectric constant g, which defines the voltage response in open circuit condition as a function of the mechanical strain, helps determining the inter-electrode distance. A sample of different piezoelectric materials, together with their coupling coefficients and mechanical quality factors are presented in Table 1. PZT ceramics, which are actually the most common piezoelectric materials, exhibit good properties for energy harvesting. Soft ceramics have high coupling coefficients and moderate mechanical quality factors, whereas hard ceramics have lower coupling coefficients and higher mechanical quality factors. Soft and hard ceramics have roughly the same figure of merit k^2Q_m, but higher stress levels tolerated by hard materials lead to higher power densities. Electromechanical properties of the PZT thin-films developed for MEMS (Micro Electro Mechanical Systems) applications are very near to bulk ceramics properties [18]. Of particular interest within this context is one of the first PZT MEMS power-generating devices developed by Jeon et al. [6]. Outstanding coupling coefficients of PMN-PT single crystals and their high quality factors enable to get very high power densities [2]. However these materials are significantly more expensive than ceramics. PVDF polymers have relatively low figure of merit, but their mechanical flexibility enables particular applications such as submarine “energy harvesting eels” [22]. Similar mechanical flexibilities and better electromechanical couplings can be reached with PZT fibre composites. Industrial manufacturing of such composites is not very developed yet, but it is expected to expand in the near future under the increasing demand of the automotive and aerospace industry.

Table 1 Coupling coefficient and mechanical quality factor for different materials.

Piezoelectric material	k_{33}	k_{31}	Q_m
PZT soft ceramic	0.75	0.64	100
PZT hard ceramic	0.68	0.57	>1000
PMN-0.25PT ceramic	0.67	0.31	280
PMN-0.25PT single crystal	0.93 (1)	0.75 (2)	360
$BaTiO_3$	0.70	0.59	400
PVDF	0.20	0.12	10
Quartz	0.15	0.1	10^4-10^6

(1) <001> oriented, *(2)* <110> oriented and <010> vibration axis

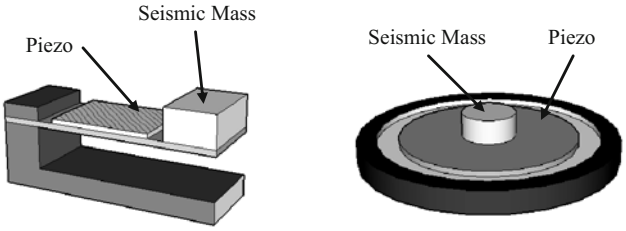

Fig. 1 Cantilever and circular membrane PEGs structures

3 Electromechanical structures

Transmission of ambient mechanical energy to the active material of PEGs is mainly envisioned through resonant mechanical structures. Indeed, such structures enable to subject relatively high stress magnitudes on the active material while minimizing the dimensions of the devices. Simplest electromechanical resonators are based on cantilever structures with piezoelectric inserts bonded on one side (unimorph) or on both sides (bimorph) [6, 7, 19–21, 23]. Resonators using circular membranes are also frequently described in literature [8, 9, 15] (Fig. 1). These structures can be modelled by the single degree of freedom {spring, mass, damper} resonator represented on Fig. 2, whose mechanical parameters are the viscous damper C_V, the structure stiffness K_S and the dynamic mass M. In general, such model represents relatively faithfully the

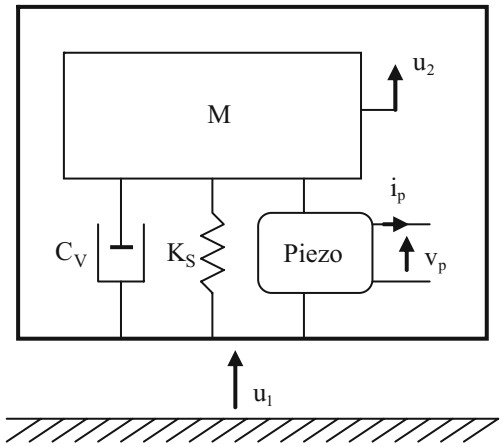

Fig. 2 SDOF model for single mode excitation

resonator behaviour near a resonance frequency. Practically, the advantage of energy harvesters coupled through resonators structures is that they may be manufactured independently to the host structure. If necessary, they can be housed into hermetic packages. Moreover they can be easily replaced in case of malfunction. On the other hand, their main drawback is their narrow frequency band, which must be tuned accordingly with the spectrum of the vibration source. Solving this problem can be relatively simple for applications with stable and well known vibration frequency, for instance in the case of vibrations generated by machine tools equipped with 50 or 60 Hz electrical motors. The resonance frequency of the generator may be tuned by changing the attached proof mass. But this mass also influences the generator sensitivity. Geometry and electromechanical properties of the materials have been investigated in particular in the case of cantilever structures [14, 15, 20].

There is another way to consider PEGs design, with direct use of stress/strain variations of the vibrating host structure. In this case, the microgenerators are not limited to operations at specific resonance frequencies, since the frequency spectrum of mechanical strain/stress transmitted to the active material is a direct image of the strain variations in the host structure. Therefore the frequency spectrum may be truly broadband for this PEG category. Thus, random environmental vibrations will not have the same effect and will not be harvested in the same way as in the case of resonant PEGs [12].

Electromechanical behaviour of the structures may be more or less simply modelled. In the simplest cases based on single-mode resonant structures, an analytical model of the resonator near its resonance frequency can be derived from the single degree of freedom {spring, mass, viscous damper} resonator represented on Fig. 2. The corresponding dynamic equation is given by (1), where the mechanical displacement u is the difference of the dynamic mass displacement and the generator's base displacement u_2-u_1. Linear electromechanical coupling may be represented by a force factor α, defining the dependence of the piezoelectric force F_P with the piezoelectric voltage V_P. The force factor also defines the relation of the electric charge Q_P generated by the piezoelectric element with the mechanical displacement u (Eq. 2). C_0 is the blocking capacitance of the piezoelectric element. Such an electromechanical model may represent more or less faithfully the behaviour of resonant microgenerators, depending on the nonlinearities of the actual systems.

$$M \cdot \ddot{u} + C_V \cdot \dot{u} + K \cdot u + F_P = M \cdot \ddot{u}_1 \tag{1}$$

$$\begin{cases} F_P = \alpha \cdot V_P \\ Q_P = \alpha \cdot u - C_0 \cdot V_P \end{cases}. \tag{2}$$

4 Power interfaces

The general structure of the power conversion chain can be divided into three different interfaces, as represented on Fig. 3. The piezoelectric element of the microgenerator subjected to strain/stress variation generates alternate voltage. This piezoelectrically induced alternate voltage V_P needs to be rectified to enable the produced electrical energy to be used or stored. This conversion is realized by an AC–DC converter, so called "Interface 1", which can be for instance a diode bridge rectifier. One-stage power interface includes Interface 1 only. Optimization of the power flow requires an adaptation of the rectified voltage respectively with the mechanical displacement magnitude.

Fig. 3 Power interfaces

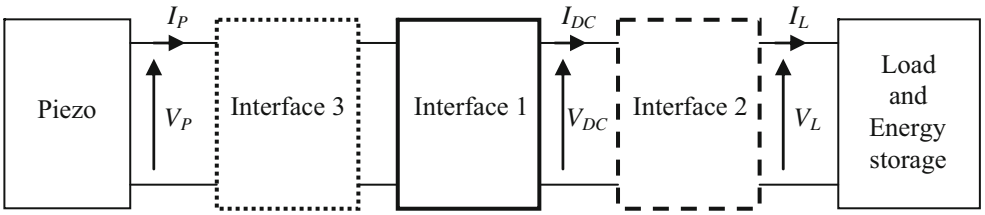

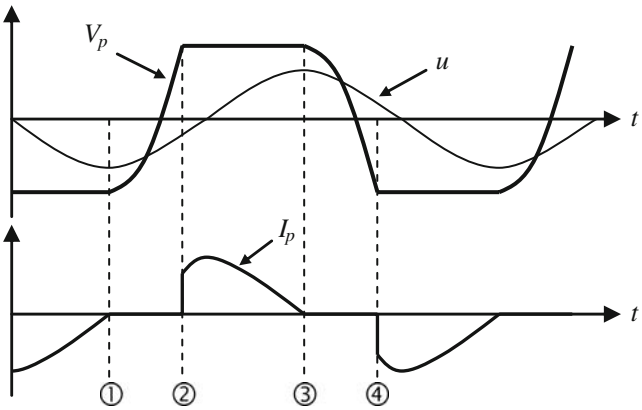

Fig. 4 Typical waveforms with one-stage and two-stage power interfaces

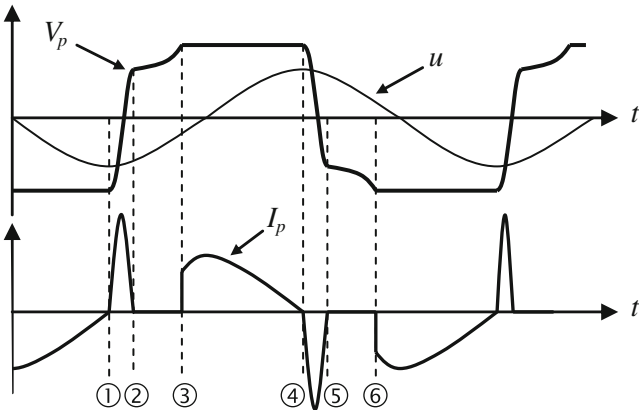

Fig. 6 Typical waveforms with the three-stage power interface (Parallel-SSHI)

This function is achieved by the so called "Interface 2", which can be for example implemented using a DC/DC converter [13, 16, 17]. The two-stage power interface is typically composed of the Interfaces 1 and 2. An additional interface, so called "Interface 3", can be used for increasing the power produced by the piezoelectric element, by performing an original non-linear treatment on the piezoelectric element voltage [1, 2, 4, 5, 10–12]. The Three-stage power interface thus includes Interfaces 1, 2 and 3.

The energy conversion cycles of the active material are determined in particular by the nature of the power interface used. Waveforms and energy analysis are presented here in the case of sinusoidal mechanical displacement u with an amplitude U_M. Waveforms with one-stage and two-stage power interfaces have similar shapes. In these cases, typical mechanical displacement, piezoelectric voltage and current waveforms are represented on Fig. 4. The four limits of the energy conversion cycle are numbered on this figure: between ① and ② the piezoelectric element is in open circuit and its voltage varies respectively with the mechanical displacement; between ② and ③ the rectifier conducts and the piezoelectric voltage is held at the DC voltage value; between ③ and ④ the piezoelectric element is in open circuit; finally, between ④ and ① the rectifier conducts and the piezoelectric voltage is held at minus the DC voltage value. The corresponding energy conversion cycle of Q_P as a function of V_P is represented on Fig. 5. The energy converted per cycle by the active material W_{conv} can be calculated using Eq. 3, where Q_P is the electric charge outgoing from the piezoelectric electrodes. Equations 2, 3 and the waveforms of Fig. 4 lead to the expression 4 of the energy $W_{one\text{-}stage}$ converted per cycle as a function of the magnitude U_M of the mechanical displacement and the rectified voltage V_{DC} with the one-stage power interface. One can deduce from this expression that $W_{one\text{-}stage}$ is maximum under the condition that V_{DC} equals $\alpha \cdot U_M/2C_0$. This clarifies the exact role of the Interface 2 used in the two-stage power interface, where the DC–DC power converter is used for varying the voltage V_{DC} proportionally to the displacement

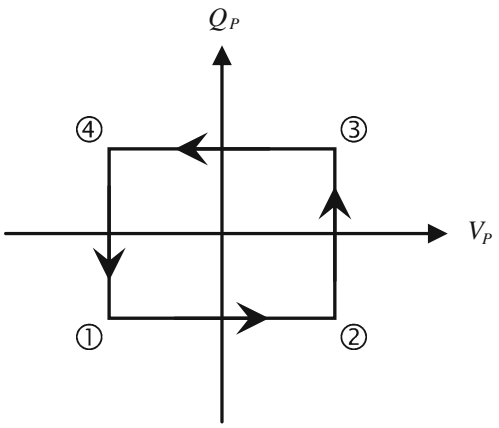

Fig. 5 $Q_P(V_P)$ energy cycle with one-stage and two-stage power interfaces

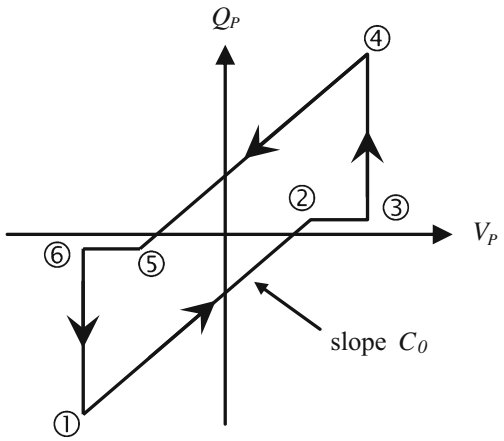

Fig. 7 $Q_P(V_P)$ energy cycle with three-stage power interface (Parallel-SSHI)

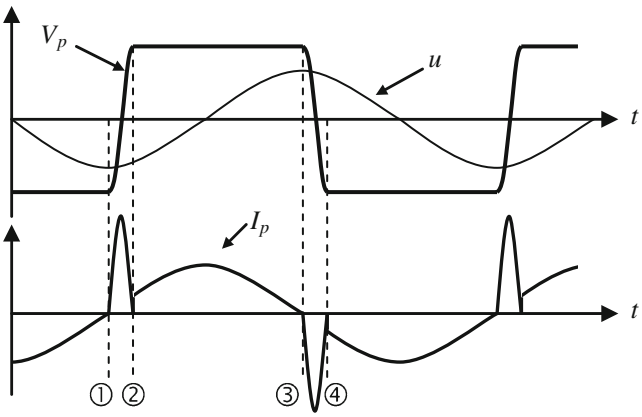

Fig. 8 Typical waveforms in the case of Ericsson cycles

magnitude. In other words, Interface 2 ensures the maximal power point tracking of the device composed of the electromechanical structure and Interface 1. Thus, with the two-stage interface the expression of the energy converted per cycle by the active material $W_{\text{two-stage}}$ is given by Eq. 5.

$$W_{\text{conv}} = \int_{\text{cycle}} V_{\text{P}} \cdot I_{\text{P}} \cdot \mathrm{d}t = \int_{\text{cycle}} V_{\text{P}} \cdot \mathrm{d}Q_{\text{P}} \tag{3}$$

$$W_{\text{one-stage}} = 4C_0 \cdot V_{\text{DC}} \left(\frac{\alpha}{C_0} U_{\text{M}} - V_{\text{DC}} \right) \tag{4}$$

$$W_{\text{two-stage}} = \frac{\alpha^2}{C_0} U_M^2 \tag{5}$$

The waveforms presented on Fig. 6 correspond to the three-stage Interface, with the so-called "Parallel-SSHI" technique used as Interface 3. By principle, the role of the Parallel-SSHI consists in reversing the piezoelectric voltage each time the mechanical displacement reaches an extremum. The circuit operating this voltage reversal induces energy losses characterized by the factor γ ($0<\gamma<1$). The six limits of the energy conversion cycle are numbered on Fig. 6: between ① and ② the piezoelectric voltage is quickly reversed by the Parallel-SSHI from $-V_{\text{DC}}$ to $+\gamma V_{\text{DC}}$; between ② and ③ the piezoelectric element is let in open circuit; between ③ and ④ the rectifier conducts and the piezoelectric voltage is held at $+V_{\text{DC}}$; between ④ and ⑤ the piezoelectric voltage is quickly reversed by the Parallel-SSHI from $+V_{\text{DC}}$ to $-\gamma V_{\text{DC}}$; between ⑤ and ⑥ the piezoelectric element is in open circuit; finally, between ⑥ and ① the rectifier conducts and the piezoelectric voltage is held at $-V_{\text{DC}}$. The corresponding energy conversion cycle of Q_{P} as a function of V_{P} is represented on Fig. 7. Equations 2, 3 and the waveforms of Fig. 6 lead to the expression 6 of the energy $W_{\text{Parallel-SSHI}}$ converted per cycle by the active material using the Parallel-SSHI interface. The first term of this expression corresponds to the useful part of the converted energy, that is to say the electrical energy which can effectively be harvested. The second term corresponds to the energy dissipated into the Parallel-SSHI circuit, composed of an electronic switch in series with an inductor. According to Eq. 6, the useful part of the converted energy reaches a maximum when V_{DC} is adjusted at the optimal value $\alpha \cdot U_{\text{M}}/(C_0(1-\gamma))$. Equation 6 shows in particular that for a given displacement magnitude the useful energy may be highly increased using the Interface 3, under the condition that the Interface 2 adjusts the V_{DC} voltage to its optimal value. Thus, in the case of a three-stage interface using the Parallel-SSHI

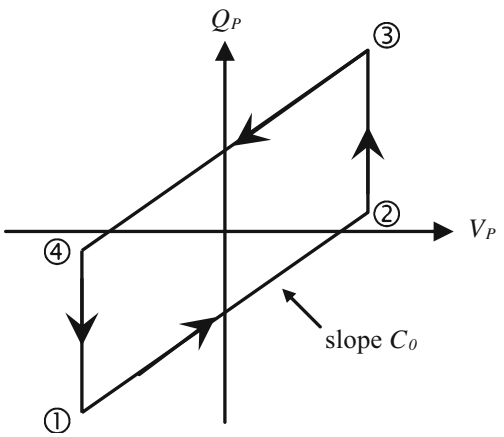

Fig. 9 $Q_{\text{P}}(V_{\text{P}})$ Ericsson energy cycle

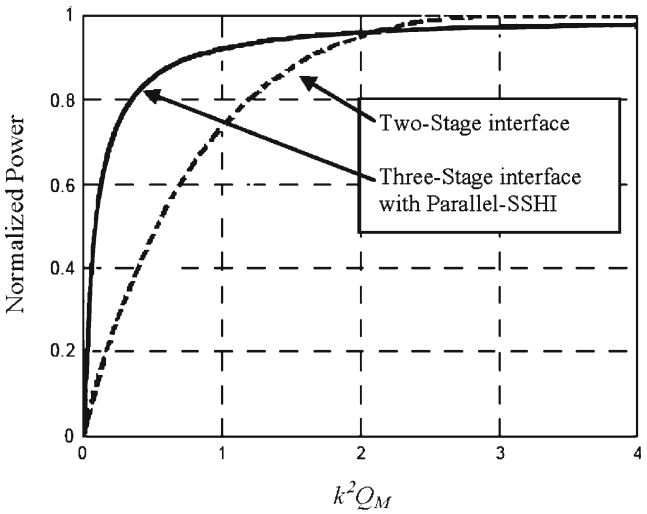

Fig. 10 Powers with the two-stage and the three-stage interfaces as a function of the figure of merit

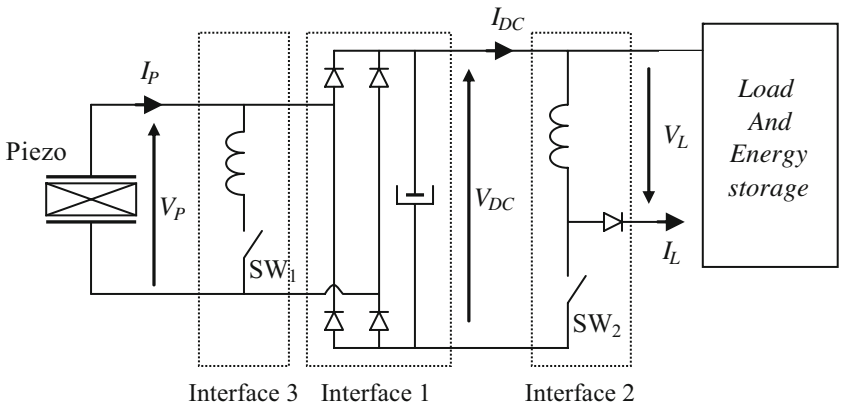

Fig. 11 Example of practical implementation for the three-stage power interface

circuit as Interface 3, the useful part of the energy converted per cycle by the active material $W_{\text{three-stage}}$ is given by Eq. 7.

$$W_{\text{Parallel-SSHI}} = 2C_0 \cdot V_{\text{DC}}\left(\frac{2\alpha}{C_0}U_{\text{M}} - V_{\text{DC}}(1-\gamma)\right) + C_0 \cdot V_{\text{DC}}^2(1-\gamma^2) \quad (6)$$

$$W_{\text{three-stage}} = \frac{2\alpha^2}{C_0(1-\gamma)}U_{\text{M}}^2 \quad (7)$$

The novelty in this paper consists in envisioning energy conversion cycles as Ericsson thermodynamic cycles. In this case, the typical voltage and current waveforms are those of Fig. 8. The four limits of this energy conversion cycle are numbered on this figure: between ① and ② the piezoelectric voltage is quickly reversed from $-V_{\text{DC}}$ to $+V_{\text{DC}}$; between ② and ③ the piezoelectric voltage is held at $+V_{\text{DC}}$; between ③ and ④ the piezoelectric voltage is quickly reversed from $+V_{\text{DC}}$ to $-V_{\text{DC}}$; finally, between ④ and ① the piezoelectric voltage is held at $-V_{\text{DC}}$. Thus, contrarily to the previous cases, the piezoelectric element is never left in open circuit. The corresponding energy conversion cycle of Q_{P} as a function of V_{P} is represented on Fig. 9. The expression of the energy W_{Ericsson} converted per cycle is given in Eq. 8. Contrarily to the previous energy expression, the energy per cycle doesn't depend on the blocking capacitor C_0. This is due to the principle of the Ericsson cycle, in which the V_{DC} value is imposed by the processing interface independently to the other parameters. According to this modelling, the energy converted by cycle is proportional to the voltage V_{DC}, which can theoretically be any value. In practice, this voltage is limited by the maximum electric field tolerated by the considered piezoelectric material. However, Ericsson cycles are an interesting way for increasing the energy converted per cycle. One can notice that Ericsson cycles potentially enable a more important increase of the energy converted than the Parallel-SSHI technique.

$$W_{\text{Ericsson}} = 4\alpha \cdot U_{\text{M}} \cdot V_{\text{DC}} \quad (8)$$

Whatever the power interface used, extracting energy from vibrations may induce mechanical damping. This is

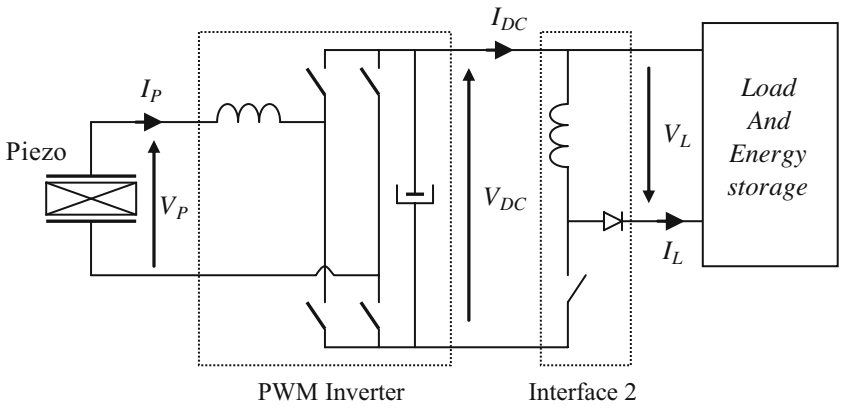

Fig. 12 Example of practical implementation for Ericsson energy conversion cycles

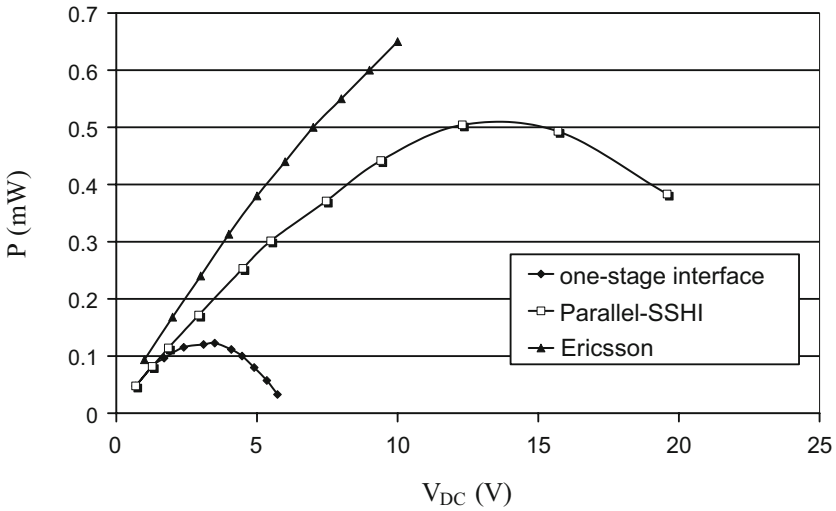

Fig. 13 Powers as a function of the V_{DC} voltage with 1.8 mm displacement magnitude of the beam free-end

particularly noticeable in the case of structures with high electromechanical coupling, such as most of the resonant PEGs structures presented in Section 3. As a consequence, the displacement magnitude U_M may be attenuated and the energy converted per cycle too. The damping effect induced by the energy harvesting process can be calculated using a model of the coupled structure such as that which is analytically modelled by Eq. 1. Figure 10 shows for instance a comparison of the powers converted using the two-stage and the three stage power interfaces (including the Parallel-SSHI) as a function of the figure of merit of the electromechanical part of the generator modelled by Eq. 1. These curves show that the three-stage interface enables the piezoelectric material to convert much more power than the two-stage interface for weak values of the figure of merit. The powers reach the same value for $k^2Q_M=2$, and one can conclude that Interface 3 does not improve anymore the energy conversion above this value.

5 Practical implementation

There are several possibilities for achieving the AC–DC conversion of Interface 1, but one of the simplest is the four diode rectifier bridge with a voltage smoothing capacitor represented on Fig. 11. The proposed Interface 2 is a "Buck-Boost" type DC–DC switching mode power converter [13]. This circuit is frequently used in systems requiring power management interfaces. It is peculiarly interesting for the presented application, first because the way to controlling the electronic switch SW_1 for tuning V_{DC} at the optimal value is particularly simple [7], and then because the input voltage V_{DC} can be either lower or higher than the output voltage V_L. Indeed, if ambient vibrations have large magnitude variations, the optimal voltage V_{DC} varies consequently, whereas the load voltage must be kept constant in general. The Interface 3 presented on Fig. 11 is the Parallel-SSHI, whose operation principles and practical

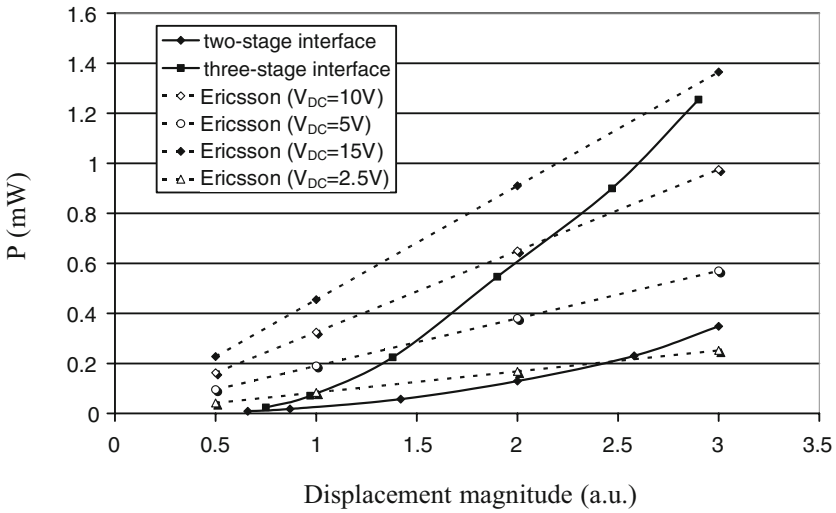

Fig. 14 Powers as a function of the displacement magnitude for the different interfaces

implementation have been presented in previous papers [1, 2, 4, 10–12].

There are also several possible circuits for achieving Ericsson cycles. The circuit presented on Fig. 12 is a PWM (Pulse Width Modulation) AC–DC power converter, whose principle of operation is detailed in particular in [3]. An additional DC–DC converter (Interface 2) can be used for adaptation of the voltage V_L to the terminal load requirement.

The experimental comparison of the presented interfaces is made using an electromechanical setup composed of a cantilever piezoelectric bimorph whose vibration is driven at 105 Hz by a function generator through a miniature electromagnet. The steel beam dimensions are $0.3\times10\times50$ mm^3, and the two PZT inserts bonded on each side of the steel beam have dimensions of $0.15\times0.9\times30$ mm^3. The experimental results presented on Fig. 13 verify a well known result: the power converted by the piezoelectric element is higher with the Parallel-SSHI processing circuit than with the one-stage power interface for the same displacement magnitude of 1.8 mm of the bimorph free-end. And the powers variations as a function of V_{DC} verify Eq. 4 and 6. An interesting point is that the power converted by the piezoelectric element is higher in the case of the Ericsson energy conversion cycles than in the case of the two other interfaces. And this power increases quasi-linearly with the V_{DC} voltage, following the theoretical behavior which can be deduced from Eq. 8. The experimental results presented on Fig. 14 show that the powers of the two-stage and three-stage interfaces vary roughly with the displacement magnitude squared, verifying the theoretical behaviors which can be deduced from Eqs. 5 and 7. For a given value of V_{DC}, the power converted using Ericsson cycles varies linearly with the mechanical displacement magnitude. This linear behavior can be theoretically deducted from Eq. 8. The fundamental difference between the two-stage or the three-stage power interface and the Ericsson cycle is that, in this last case, the optimal V_{DC} can not be derived from the presented energy analysis. However, an optimal V_{DC} value could be derived from the overall dynamic model of the considered device, taking into account the damping effect induced by the energy conversion process.

These experimental results confirm the interest of using Ericsson cycle for increasing the energy converted by piezoelectric materials. And thus, using this principle could be profitable for improving the performances of miniature vibration-powered piezoelectric electrical generators. From the practical point of view, the proposed power interfaces must have very weak losses and their control circuitry must consume very little electrical power. With these considerations, practical implementation of the electronic circuitry is not easy using discrete components if the power converted remains below a milliwatt. For very low power levels, conception of specific integrated circuits seems to be a promising way to get high efficiency power interfaces [24].

6 Conclusion

Theoretical and experimental results presented in this paper show that the two-stage and the three stage electrical interfaces enables a better use of the piezoelectric material for converting mechanical energy into electrical energy compared to the one-stage interface. Moreover, the three-stage interface may bring a significant increase of the power converted, in particular in the case of generators having weak electromechanical figures of merit. The application of Ericsson thermodynamic cycle to piezoelectric energy conversion proposed in this paper is a promising way, since the power gain is potentially higher than those of the two-stage and the three-stage interface. From the practical point of view, design and implementation of these interfaces using electronic circuits is a point to consider carefully. Indeed, the levels of harvested power remain relatively weak, generally below a milliwatt, and thus there is a need for particular control circuits with extremely low consumption associated to power circuits with moderate losses in order to get high efficiency miniature vibration-powered piezoelectric electrical generators.

Reference

1. A. Badel, E. Lefeuvre, C. Richard, D. Guyomar, J. Intell. Mater. Syst. Struct. **16**(10), 889 (2005)
2. A. Badel, A. Benayad, E. Lefeuvre, L. Lebrun, C. Richard, D. Guyomar, IEEE Trans. Ultrason. Ferroelectr. Freq. Control. **53**, 673 (2006)
3. R.W. Erickson, D. Maksimoviâc, *Springer ed.*, ISBN 0792372700 (2001)
4. D. Guyomar, A. Badel, E. Lefeuvre, C. Richard, IEEE Trans. Ultrason. Ferroelectr. Freq. Control. **52**, 584 (2005)
5. D. Guyomar, Y. Jayet, L. Petit, E. Lefeuvre, T. Monnier, C. Richard, M. Lallart, Sensors and Actuators A, **138**(1), 151 (2007)
6. Y.B. Jeon, R. Sood, J.H. Jeong, S.G. Kim, Sens. Actuators A, **122**, 16 (2005)
7. A. Kasyap, J. Lim, K. Ngo, A. Kurdila, T. Nishida, M. Sheplak, L. Cattafesta, presented at the *Ninth International Congress on Sound and Vibration* (2002)
8. S. Kim, W.W. Clark, Q.M. Wang, J. Intell. Mater. Syst. Struct. **16**, 847 (2005)
9. S. Kim, W.W. Clark, Q.M. Wang, J. Intell. Mater. Syst. Struct. **16**, 855 (2005)
10. E. Lefeuvre, A. Badel, C. Richard, D. Guyomar, J. Intell. Mater. Syst. Struct. **16**(10), 865 (2005)
11. E. Lefeuvre, A. Badel, C. Richard, D. Guyomar, Sens. Actuators A. **126**(2), 405 (2006)
12. E. Lefeuvre, A. Badel, C. Richard, D. Guyomar, Journal of Electroceramics, online first (2006)
13. E. Lefeuvre, D. Audigier, C. Richard, D. Guyomar, IEEE Trans. Power Electron. **22**, 2018 (2007)

14. F. Lu, H.P. Lee, S.P. Lim, Smart Mater. Struc. **13**, 57 (2004)
15. E. Minazara, D. Vasic, F. Costa, Ultrasonics. **44**, 699 (2006)
16. 5. G.K. Ottman, H.F. Hofmann, G.A. Lesieutre, IEEE Trans. Power Electron. **18**, 696 (2003)
17. 6. G.K. Ottman, H.F. Hofmann, A.C. Bhatt, G.A. Lesieutre, IEEE Trans. Power Electron. **17**, 669 (2002)
18. N. Setter, in *Piezoelectric materials in devices*, ISBN 2-9700346-0-3, (2002)
19. S. Roundy, P.K. Wright, Smart Mater. Struc. **13**, 1131 (2004)
20. Y.C. Shu, I.C. Lien, J. Micromechanics Microengineering. **16**, 2429 (2006)
21. Y.C. Shu, I.C. Lien, Smart Mater. Struc. **15**, 1499 (2006)
22. G.W. Taylor, J.R. Burns, S.A. Kammann, W.B. Powers, T.R. Welsh, IEEE J. Oceanic Eng. **26**, (2001)
23. C.-N. Xu, M. Akiyama, K. Nonaka, T. Watanabe, IEEE Trans. Ultrason. Ferroelectr. Freq. Control. **45**, 1065 (1998)
24. S. Xu, K.D.T. Ngo, T. Nishida, G.-B. Chung, A. Sharma, Proc. 20th Annu. Appl. Power Electron. Conf. and Exposition. **1**, 226 (2005)